



Prediction of the joint action of binary mixtures based on characteristic parameter $k \cdot EC_x$ from concentration-response curves

Na Wang^{a,*}, Ruru Sun^a, Xiaoyan Ma^b, Xiaochang Wang^b, Jinhong Zhou^c

^a College of Architecture and Civil Engineering, Xi'an University of Science and Technology, Xi'an 710054, Shaanxi, China

^b Key Laboratory of Northwest Water Resource, Environment and Ecology, MOE, Engineering Technology Research Center for Wastewater Treatment and Reuse, Key Laboratory of Environmental Engineering, Shaanxi Province, Xi'an University of Architecture and Technology, Xi'an 710055, Shaanxi, China

^c College of Geography and Environment, Baoji University of Arts and Sciences, Baoji, Shaanxi 721013, China

ARTICLE INFO

Edited by: Caterina Faggio

Keywords:

Characteristic parameter $k \cdot EC_x$
The mode and strength of joint action
IA
 $rMDR_x$
Exponential function

ABSTRACT

The evaluation of joint toxicity of mixtures is an important topic in toxicology. Previous studies have found that the parameter $k \cdot EC_x$ of concentration response curves (CRCs) can be used to assess the applicability of concentration addition model (CA). This study further assesses the predictability of $k \cdot EC_x$ on the joint toxicity evaluation. The toxicities of the twelve environmental pollutants, as well as those of binary mixtures with an equivalent-effect concentration ratio, to *Vibrio fischeri* were determined by using the microplate toxicity analysis. The toxicity evaluation of mixtures was conducted by CA and independent action model (IA). The relationship between the joint toxicity (measured by the relative model deviation ratio ($rMDR$)) and the $k \cdot EC_x$ was studied. The results shows that the $k \cdot EC_x$ could reflect the shape of CRCs in the whole concentration range. According to the IA and CA, 65% of the mixtures produce strong antagonistic or synergistic effect due to the significant difference of $k \cdot EC_x$. The percentage of the relative difference of $k \cdot EC_x$ of components and the $rMDR_x$ can be fitted by an exponential function. Different types of interactions could be described using this function. It is suggested that the joint toxicity of binary mixtures can be assessed with the parameter $k \cdot EC_x$, which can quickly get very important data when planning experiments, but also reduce the number of experiments.

1. Introduction

A variety of exogenous substances, such as pharmaceuticals, plasticizers, personal care products, pesticides and so on, are poured into the water body, seriously threatening the sustainability of water ecological function and human health. A large number of studies have shown that the joint toxicity of mixtures to all levels of organisms in water is often greater than the sum of the toxicity of single substances (Arrhenius et al., 2004; Hass et al., 2007). Evaluation of antagonistic or synergistic effects between substances is a necessary condition for accurate assessment of environmental risk, which has attracted the attention of researchers.

From the perspective of toxicology, some researchers have analyzed the mechanism of action between poisons and receptors, so as to reveal the joint toxicity of the mixtures. For example, heavy metal ions can bind to the sulfhydryl protein of bacteria to affect the division of bacteria. They can also damage the cell wall and photosynthesis of algae. Due to the same target site, most of heavy metal mixtures have synergistic effect at low concentration and antagonistic effect at high

concentration due to the competition of target site (Wang et al., 2018). Tetracycline antibiotics can cause the degradation of SecY in the transporter complex, resulting in protein congestion, inhibiting all protein secretion and causing cell death (Wu et al., 2010). But for a large number of chemical substances, the currently established mechanism of action is only the tip of the iceberg. It is more difficult to analyze the joint effect of different mechanism substances on organisms.

Therefore, more and more researchers studied how to predict the toxicity of mixtures from the perspective of modeling. Among them, the most widely used are two models: the concentration addition model (CA) and the independent action model (IA). CA and IA models get better prediction results in different situations (Bellas, 2008; Rial et al., 2013). The two models respectively describe the extreme phenomenon of mixture interaction, which may divert from what is true about mixture (Kortenkamp et al., 2009). Cedergreen et al. (2008) selected 158 binary mixtures for toxicity prediction, half of whose toxicity could not be well predicted by IA and CA. If the CRCs of individual component in the mixtures do not cover the entire range of effects, the CA model will

* Corresponding author.

E-mail address: wangna811221@xust.edu.cn (N. Wang).

<https://doi.org/10.1016/j.ecoenv.2021.112155>

Received 11 November 2020; Received in revised form 7 March 2021; Accepted 13 March 2021

Available online 20 March 2021

0147-6513/© 2021 The Authors.

Published by Elsevier Inc.

This is an open access article under the CC BY-NC-ND license

(<http://creativecommons.org/licenses/by-nc-nd/4.0/>).

have some predictive blind spots (Liu et al., 2013).

Consequently, a number of improved IA and CA models emerged. Olmstead and LeBlanc (2005) classified the substances according to the mechanism of action (MOA). Firstly, the CA model was used to calculate the joint toxicity of the substances with similar MOA. Then the IA model was used to calculate the joint toxicity of the substances with dissimilar MOA. The model is named the Two-Stage Prediction (TSP) which can well predict the joint toxicity of mixtures at the environmental concentration level. Mwense et al. (2004) adopted molecular descriptors and fuzzy set theory to characterize the degree of similarity and dissimilarity of mixture constituents and integrated the CA and IA models, establishing the Integrated Fuzzy Concentration addition - Independent action Model (INFCIM) which has more accurate prediction ability than TSP (Wang et al., 2009). The TSP and INFCIM are potentially ineffective since MOAs of many components are still uncertain. Qin et al. (2011) integrated CA with IA based on the multiple linear regression model (ICIM) for toxicity prediction of mixtures without interaction. This model showed better prediction ability than IA and CA models. Ge et al. (2014) have proved that ICIM model can predict the toxicity of mixtures that produce interaction, which further expands the application scope of the model. Qin et al. (2015) established a linear regression CA model (LCA) and a linear regression IA model (LIA), which were used to predict the toxicity of mixtures with interaction. Qin et al. (2017) further applied LCA and LIA models to the toxicity prediction of mixtures without interaction. Wang et al. (2018) established an extended concentration addition model (e-CA) which has better predictability than CA. However, the calculation of the above models are complex, and their application is far less popular than CA and IA.

Chemometrics also plays a unique role in the prediction of mixed toxicity. The quantitative structure-activity relationship (QSAR) is the most common calculation model (Kar and Leszczynski, 2019). Yao et al. (2013) predicted the mixed toxicity of different types of binary mixtures to *P. phosphoreum* by molecular docking-based binding energy. Mo et al. (2015) used the electronegativity distance vector to describe the molecular characteristics of 30 organophosphorus compounds and successfully predicted the mixed toxicity of the above chemicals to *steelhead trout*. Qin et al. (2018) used genetic algorithm to select the best theoretical descriptor, and established a QSAR evaluation model for the toxicity of binary and multivariate mixtures of two antibiotics and four pesticides to *luminescent bacteria Vibrio fischeri*. Compared with IA and CA models, the prediction accuracy of QSAR model is greatly improved. The QSAR model provide strong support for environmental risk assessment of water bodies. However, limited applicability domain and small training set restrain the utilization of QSAR, and CA and IA models cannot be completely replaced.

Our previous work found that the parameter $k \cdot EC_x$ of concentration response curves (CRCs) could be used as a control index to assess the applicability of CA model. This study promoted the development of the CA model to the actual prediction model (Wang et al., 2015a). The CRCs of substance directly reflects the action relationship between the tested organism and the exposed toxicants on a certain toxic endpoint. It may be closely related to its mechanism of action. The binary mixtures of five different types of substances were studied in the early stage. The binary mixtures with the same curve type showed additive effect. Among the binary combinations with different curve types, 71.4% of the combinations had synergistic or antagonistic effects (Wang et al., 2018). Dou et al. (2010) studied the joint action of binary mixture with J-type and S-type CRCs, and found that the mixtures showed antagonistic effect at different concentration levels. Brezovšek et al. (2014) studied the toxic effects of binary mixtures of antitumor drugs with different CRCs on *Selenastrum.sp* (Chlorophyta) and *Synechococcus* (Gloeotrichia), and found that there were synergistic or antagonistic effects to a large extent. It can be concluded that the difference between the shapes of CRCs may be the cause of the combination effect of the mixtures.

In this study, 12 toxic substances of five types commonly detected in environment were selected (Yu et al., 2019; Zhang et al., 2015; Cui et al.,

2018; Liu et al., 2015). They include two heavy metals (zinc and cadmium), two surfactants (sodium dodecyl benzoate (SDBS) and sodium dodecyl sulfate (SDS)), two pesticides (Growth herbicide dicamba (DIC) and non-selective herbicide Diquat (DQ)), three antibiotics (tetracycline hydrochloride (TC), chloramphenicol (CAP), and polymyxin B (PLB)), one clinical medication (Diphenhydramine hydrochloride (DPH)) and two ionic liquids (1-butyl-3-methylimidazolium sulfate (IL1) and 1-dodecyl-3-methylimidazolium chloride (IL2)). The single and binary acute toxicity of the 12 chemicals to *Vibrio fischeri* was tested using the microplate toxicity analysis method. Based on the CRCs of substances, the characteristic parameters which can characterize the shape of CRCs were determined. The combined toxicity of the mixtures was evaluated by the deviation between the observed effects and the effects predicted by the CA and IA model. The strength of joint action was quantified by the relative model deviation ratio ($rMDR$). Based on the CRCs of chemicals, the relationship between the joint toxicity of substances and the shape of CRCs was studied, so as to further explore the toxicity interaction of mixtures. This study explored the joint toxicity of binary mixtures from the perspective of geometric morphology, and provided theoretical support for further research of toxicity prediction of multiple mixtures.

2. Materials and methods

2.1. Chemicals

Chemicals ZnSO₄·7H₂O (CAS 7446-20-0, analytical grade), CdCl₂·2.5H₂O (CAS 7790-78-5, analytical grade), chloramphenicol (CAP, CAS 56-75-7, > 98% purity) and diphenhydramine hydrochloride (DPH, CAS 147-24-0, > 98% purity) were purchased from sigma-Aldrich (Shanghai, China). Tetracycline hydrochloride (TC, CAS 64-75-5, > 98.0% purity), sodium dodecylbenzene sulfonate (SDBS, CAS 25155-30-0, > 95.0% purity) and sodium lauryl sulfate (SDS, CAS 151-21-3, > 97.0% purity) were purchased from TCI (Japan). Diquat (DQ, CAS 85-00-7, standards 93.4% purity) and dicamba (DIC, CAS 1918-00-9, standards 99% purity) were purchased from DR (Germany). 1-dodecyl-3-methylimidazolium chloride (IL2, CAS 114569-84-5, 99% purity) were purchased from Energy Chemical (China). 1-butyl-3-methylimidazolium sulfate (IL1, CAS 445473-58-5, 99% purity) were purchased from Alfa (USA). Polymyxin B Sulfate (PLB, CAS 1405-20-5, 95% purity) were purchased from TRC (Canada). The stock solution was prepared by dissolving in Milli-Q water and stored in the dark at 4 °C. Some physical properties are listed in Table 1. The structures of the ten organic chemicals are illustrated in Fig. S1.

2.2. Experimental design and toxicity test

The marine bacterium *Vibrio fischeri* (*V. fischeri*) used in the luminescent bacteria toxicity tests was purchased in a freeze-dried form from the China Center. The luminescence inhibition of twelve single chemical and their binary mixtures were tested using the Centrol IAPc LB960 Microplate Luminometer (Berthold Technologies Company, Germany). The concentration ratios of each of chemical in mixtures are the proportions of EC₅₀ to the total concentration (C_{mix}) of the mixture. To construct the CRC of a mixture, 12 different test concentrations in 3 parallels and 12 controls in a 96-well microplate were arranged, and the microplate test was repeated three times. The samples were exposed for 15 min. The details of the *V. fischeri* and toxicity test methods were performed as described in previous work of our research group (Ma et al., 2019). All the acute biological toxicity tests were carried out three times with different batches of bacterial suspensions. The deviation of three test results should be less than 10%.

The acute toxicity of the sample was evaluated as the inhibition value:

$$I = [(R_0 - R)/R_0] \times 100\% \quad (1)$$

Table 1
The statistic parameters of fitting function, EC₅₀, and stock of twelve selected chemicals.

Chemicals / Ion	Abbr.	M.W.	<i>a</i>	<i>b</i>	<i>n</i>	Adj.R ²	Red.Chi-S	EC ₅₀ (mg/L)	Stock (mg/L)
Zn ²⁺	Zn ²⁺	65.39	98.45	0.5	4.91	0.9976	3.83	0.50±0.02	10
Cd ²⁺	Cd ²⁺	112.41	98.08	1.6	6.50	0.9909	9.57	1.61±0.03	10
Sodium dodecylbenzene sulfonate	SDBS	348.48	121.82	55.05	5.31	0.9899	12.09	51.46±0.96	150
sodium lauryl sulfate	SDS	288.38	160.19	125.55	1.10	0.9867	12.71	61.23±5.12	1000
Diquat	DQ	344.05	111.45	627.40	3.12	0.9893	12.31	587.18±20.25	2500
Dicamba	DIC	221.04	110.26	84.04	4.06	0.9919	10.48	80.25±5.34	1000
Chloramphenicol	CAP	323.13	126.44	676.42	1.18	0.9892	6.95	454.01±17.33	2500
Tetracycline hydrochloride	TC	480.90	89.39	78.78	4.81	0.9957	4.67	82.81±5.99	1000
Polymyxin B Sulfate	PLB	1301.56	79.87	2.37	2.28	0.9957	2.80	3.03±0.05	100
Diphenhydramine hydrochloride	DPH	291.82	163.52	650.50	1.19	0.9901	8.37	328.46±14.72	1500
1- butyl-3-methylimidazocine sulfate	IL1	348.5	101.89	510.56	1.92	0.9964	4.12	500.68±20.54	5000
1-dodecyl-3-methylimidazolium chloride	IL2	286.88	103.10	1.32	3.72	0.9901	14.69	1.28±0.03	10

M.W is molecular weight; *a*, *b* and *n* are parameter of Hill function; Adj.R² is adjusted correlation coefficient squared; Red.Chi-S is the reduced chi-squared test; EC₅₀ is 50%-effect concentration and its 95% confidence interval.

where *I*: the inhibition value; *R* and *R*₀: the average relative luminescence unit (RLU) values of the samples and the controls, respectively, after 15 min exposure. The toxicity tests were repeated three times.

The binary mixtures were a series of equal toxicity solutions (ETS) (Tan et al., 2011) prepared following the classical empirical approach with concentration levels as EC₅₀, where EC₅₀ denotes the effective concentration corresponding to an inhibition value of 50% for individual chemicals. A total of 66 binary mixture rays composed of twelve toxicants referred were designed.

2.3. Concentration response curve fitting

The experimental data were mathematically manipulated to obtain the CRCs for each individual chemical and the binary mixtures by non-linear least square (NLLS) calculation. As all the data sets were found to fit well with the Hill function, the following equation was used as a mathematical expression of the CRCs:

$$I = a \times c^n / (b^n + c^n) \quad (2)$$

where *c* (mg/L): the mass concentration, *I* (%): the inhibition as a response to *c*, *a* (%): the effect corresponding to the infinite concentration, *b* (mg/L): the concentration when the effect is *a*/2, *n* (non-dimensional): the parameter representing slope. The 95% confidence intervals (CI) of CRCs were calculated to describe experimental error and fitting uncertainty (Liu et al., 2009).

The following equation was the derivative of the Hill function that is used to calculate slope *k* of the CRCs:

$$k = I' = \frac{nab^n c^{n-1}}{(c^n + b^n)^2} \quad (3)$$

2.4. The parameter *k*·EC_x of the CRCs

The detailed derivation process of the parameter *k*·EC_x of the material CRCs is shown in the previous literature published by our research group (Wang et al., 2015). This paper only introduces the calculation process of characteristic parameters. It is known from the literature that:

$$\frac{c_i}{EC_x} = 1 - \frac{x - x_i}{k \cdot EC_x} \quad (4)$$

where (*c*_{*i*}, *x*_{*i*}), (*EC*_{*x*}, *x*) are two coordinate points on a CRC, *k* is the slope of the line which goes through the point (*c*_{*i*}, *x*_{*i*}) and (*EC*_{*x*}, *x*). It is approximately equal to the derivative of the concentration response function at the point (*EC*_{*x*}, *x*) when the point (*c*_{*i*}, *x*_{*i*}) is close to the point (*EC*_{*x*}, *x*). Any CRC fitting function has derivative function, such as the Logit and Weibull in some papers. In this paper, the derivative function of Hill equation is specially referred to, as shown in Eq. (3). The left side of Eq. (4) is the expression of CA model, and its value is directly

proportional to the value of parameter *k*·EC_x. CA model is the most widely used at present to evaluate the joint action of mixtures, so the parameter *k*·EC_x is the characteristic parameter to characterize the CRCs of substance.

2.5. Toxicity interaction evaluation

The toxicological interaction in the mixture was identified by using the CA, IA. If the toxicity predicted by CA/IA is higher than the upper 95% CI or lower than the lower 95% CI of observed toxicity, it is deemed to be antagonistic or synergistic, respectively. If the toxicity predicted by CA/IA is located between the CIs, it is considered to be additive (Chen et al., 2019). The mathematical equations of the CA model are Eqs. (5) and (6) (Altenburger et al., 2004). The strength of joint action was quantified by the relative model deviation ratio (*rMDR*) (Belden et al., 2007):

$$EC_{x,mix} = \left(\sum_{i=1}^n \frac{p_i}{EC_{x,i}} \right)^{-1} \quad (5)$$

$$\sum_{i=1}^n \frac{c_i}{EC_{x,i}} = 1 \quad (6)$$

where *EC*_{*x,mix*} represents the mixture concentration that provokes *x*% joint effect, *EC*_{*x,i*} is the concentration of the *i*th component that provokes *x*% effect when applied individually, and *p*_{*i*} refers to the ratio of the concentration of the *i*th component (*c*_{*i*}) in the mixture to the total mixture concentration (*c*_{*mix*}).

The mathematical equation of the IA model is as follows:

$$E(C_{x,mix}) = 1 - \prod_{i=1}^n (1 - E(c_i)) \quad (7)$$

where *E*(*C*_{*mix*}) refers to the total effect of the mixture, and *E*(*c*_{*i*}) denotes the effect of the *i*th component with a concentration of *c*_{*i*} in the mixture.

The mathematical equation of the *rMDR* model is as follows:

$$rMDR_x = \frac{EC_{x,pr} - EC_{x,ob}}{EC_{x,ob}} \times 100\% \quad (8)$$

where *rMDR*_{*x*} refers to the strength of joint action, and *EC*_{*x,pr*} refers to the concentration that provokes *x*% of predicted value of CA or IA, *EC*_{*x,ob*} refers to the expected value of observed concentration that provokes *x*%. The values of 95% CI calculated by using inverse Hill function were applied in *rMDR*_{*x*} and denoted as *rMDR*_{*x,up*} and *rMDR*_{*x,low*} (Chen et al., 2019). When the *rMDR*_{*x,low*} ≤ *rMDR*_{*x*} ≤ *rMDR*_{*x,up*}, the joint action is additive; when the *rMDR*_{*x*} = *rMDR*_{*x,up*} > 0, the joint action is synergistic; when the *rMDR*_{*x*} = *rMDR*_{*x,low*} < 0, the joint action is antagonistic. |*rMDR*_{*x*}| is the strength of joint action.

2.6. Fitting the relationship between $\Delta(k \cdot EC_x)\%$ and the strength of joint action

The relationship between the percentage of relative difference of characteristic parameter $k \cdot EC_x$ ($\Delta(k \cdot EC_x)\%$) and the strength of joint action was also fitted by non-linear least square method and Origin Pro 8.5 (OriginLab, North-ampton, MA, USA). 66 mixtures data can be well fitted by exponential function. The following equation was the mathematical expression of the exponential function:

$$rMDR_x = A + B e^{R_0 \cdot \Delta(k \cdot EC_x)\%} \quad (9)$$

$$\Delta(k \cdot EC_x)\% = \frac{(k \cdot EC_x)_1 - (k \cdot EC_x)_2}{(k \cdot EC_x)_1} \times 100\% \quad (10)$$

where k is the slope of CRCs at the concentration of EC_x , $(k \cdot EC_x)_1$ refers to the characteristic parameter of CRCs for component 1 of binary mixture when the concentration is EC_x , $(k \cdot EC_x)_2$ refers to the characteristic parameter of CRC for component 2 of binary mixture when the concentration is EC_x , A (%), B (Dimensionless), R_0 (Dimensionless) refers to the fitting parameters of exponential function, and $rMDR_x$ refers to the strength of joint action corresponding to $x\%$ effect of binary mixture.

The principle of defining substance 1 and substance 2 is as follows: the parameter $\Delta(k \cdot EC_x)\%$ calculated according to Eq. (10) increases from $\Delta(k \cdot EC_5)\%$ to $\Delta(k \cdot EC_{95})\%$. The purpose of this is that: Fig. 2, drawn according to Eq. (9), shows the change of the joint action of the binary mixtures (the $rMDR_x$) from low to high concentration. $|\Delta(k \cdot EC_x)\%|$ measures the difference in the shape of CRCs between components of binary mixtures. The positive or negative change of $\Delta(k \cdot EC_x)\%$ indicates the change in the trend of CRC of substance 1 and substance 2.

3. Results and discussion

3.1. The CRCs of individual chemicals selected

The Hill function (Eq. (3)) was used to fitting the CRCs of the twelve chemicals towards *V. fischeri*. Table 1 lists the relevant parameters of fitting results for the selected individual chemicals. As all the $Adj.R^2$ values were higher than 0.98 and the $Red.Chi-S$ values were lower than 15, it could be concluded that the experimental data were well fitted by the Hill function. According to the mass concentrations corresponding to EC_{50} to evaluate the toxicity, the most toxic chemical is Zn^{2+} and the least toxic chemical is Diquat (DQ). The toxicity order of the selected chemicals is $Zn^{2+} > 1$ -dodecyl-3-methylimidazolium chloride (IL2) $> Cd^{2+} > Polymyxin B Sulfate (PLB) > Sodium dodecylbenzene sulfonate (SDBS) > sodium lauryl sulfate (SDS) > Dicamba (DIC) > Tetracycline hydrochloride (TC) > Diphenhydramine hydrochloride (DPH) > Chloramphenicol (CAP) > 1$ -butyl-3-methylimidazocine sulfate (IL1) $> Diquat (DQ)$. Among them, the acute toxicity of heavy metals to *V. fischeri* is the highest. The toxicity of ionic liquids varies greatly. The toxicity of IL2 is 391 times that of IL1. Both of them are methyl imidazole ionic liquids, and their toxicity depends on the characteristics of substituents, which was also found in early studies (Diaz et al., 2018). The toxicity of the two surfactants was not significantly different. The acute toxicity of SDBS is 1.19 times that of SDS, indicating that the toxicity of substituted benzenesulfonic group is slightly higher than that of sulfato group. Among the three antibiotics, PLB exhibits the strongest biological toxicity, with EC_{50} of 3.03 mg/L, which is 27.3 times and 149.8 times the toxicity of TC and CAP, respectively. This result is consistent with PLB as the last resort to deal with bacteria (Zhan et al., 2019). DQ and DIC show weak acute toxicity to bacteria. However, the toxicity of selective herbicide (DICIC) to *V. fischeri* is 6.3 times higher than that of non-selective herbicide (DQ). The twelve CRCs of the selected chemicals are plotted in Fig. S2. The value of parameter n reflects the trend of the curves to a certain extent. The larger the value of n

(such as Zn^{2+} , Cd^{2+} , SDBS, DQ, DIC, IL2, TC, the value of n varying from 3.12 to 6.50), the greater the slope of the middle section of the curve. While the values of n (such as SDS, IL1, DPH, CAP, PLB) are all close to 1, so the slopes in the middle of these curves are close to each other.

3.2. Characteristic parameter $k \cdot EC_x$ for characterizing the shape of CRCs

The parameters $k \cdot EC_x$ of 12 selected reference materials are listed in Table 2. It can be seen from Table 2 that the $k \cdot EC_x$ of CRCs for 12 substances are quite different. Taking $k \cdot EC_{50}$ as an example, the parameter of Cd^{2+} is 159.4, while that of CAP is 36.3. The $k \cdot EC_{50}$ of Cd^{2+} is 4.4 times as much as that of CAP. The $k \cdot EC_x$ of the same substance also varies greatly in the whole concentration range. Taking SDBS as an example, its $k \cdot EC_5$ is 25.4, and $k \cdot EC_{60}$ is 161.3, the difference between them being 5.4 times. According to Table 1 and Table 2, the variation trend of fitting parameter n of the dose-effect equation is $Cd^{2+} > SDBS > Zn^{2+} > TC > DIC > IL2 > DQ > PLB > IL1 > DPH > CAP > SDS$, and the variation trend of parameter $k \cdot EC_{50}$ is $Cd^{2+} > SDBS > Zn^{2+} > DIC > TC > IL2 > DQ > IL1 > PLB > DPH > SDS > CAP$. The order of the two is basically the same, with slight changes in some parts. It can be seen from Section 3.1 that the value of n is related to the shape of CRCs to a certain extent, so $k \cdot EC_x$ is also a characteristic parameter that can characterize the shape of CRCs. The $k \cdot EC_x$ has its exact value corresponding to different concentrations, so it can better reflect the morphological trend of CRCs in the entire concentration interval. Among the 12 substances, CAP, DPH and SDS have similar $k \cdot EC_x$, Zn^{2+} and TC have similar $k \cdot EC_x$, indicating that their dose-effect curves have similar curve trends; otherwise, the curve trends are different.

3.3. The joint toxic effects of binary mixtures

The acute toxicity of 66 equal toxicity binary mixtures to *V. fischeri* was determined by microplate test. The CRCs of all binary mixtures can be well fitted by Hill equation. The fitting information of acute toxicity of binary mixtures is detailed in Table S1, including mixture concentration ratio, fitting parameters, $Adj.R^2$ and $Red.Chi-S$. All the $Adj.R^2$ values are greater than 0.98, the $Red.Chi-S$ values are less than 13. The CA and IA models were used to evaluate the joint effects. The CRCs of binary mixtures were compared with IA CRCs, CA CRCs to determine the joint action of binary mixtures. The joint action analysis of the whole concentration range of binary mixtures is shown in Fig. 1 and Fig. S3. It can be seen from Fig. 1 and Fig. S3 that the measured CRCs of 43 binary mixtures deviated significantly from the predicted CRCs of IA and CA, resulting in strong antagonistic or synergistic effects. 65% of the mixtures have interactions, which further verifies the previous research results of our research group, and the binary mixtures with different shape of CRCs are easy to produce interactions (Wang et al., 2018).

3.4. Toxicity evaluation using CA and IA models

It can be seen from Fig. 1 and Fig. S3 that the evaluation results of IA and CA on the joint action of binary mixtures are quite different. The CA model is applied under the assumption that mixture components have the same or similar MOA (Loewe, 1926), whereas IA is utilized under the assumption that mixture components have different MOA (Bliss, 1939). The 12 environmental chemicals selected in this paper have different sources, different chemical structures and different MOA on *V. fischeri*. The CRCs of the selected substances were quite different (parameter $k \cdot EC_{50}$ varying from 37.8 to 159.4). When the shape of CRCs of substances is quite different, CA will bring huge error to evaluate the joint effect (Wang et al., 2015). Since the maximum inhibition rate of PLB is only 70%, there will be a prediction blind area when CA model is used to evaluate the binary mixtures containing PLB (Liu et al., 2013). Therefore, the IA model is selected as the evaluation model of binary mixtures in the following sections.

The strength of the joint action was assessed by the deviation

Table 2
The characteristic parameter $k \cdot EC_x$ of CRCs for the selected individual chemicals.

Chemicals	$k \cdot EC_5$	$k \cdot EC_{10}$	$k \cdot EC_{20}$	$k \cdot EC_{30}$	$k \cdot EC_{40}$	$k \cdot EC_{50}$	$k \cdot EC_{60}$	$k \cdot EC_{70}$	$k \cdot EC_{80}$	$k \cdot EC_{90}$
Zn ²⁺	23.3	44.0	78.1	102.2	116.4	120.6	114.9	99.2	73.6	38.1
Cd ²⁺	30.8	58.4	103.5	135.4	154.0	159.4	151.5	130.3	95.9	48.3
SDBS	25.4	48.6	88.6	119.8	142.4	156.2	161.3	157.8	145.5	124.5
CAP	5.8	11.1	20.2	27.5	32.8	36.3	37.8	37.5	35.2	31.1
DPH	5.8	11.3	21.1	29.4	36.3	41.7	45.6	48.0	49.0	48.6
DQ	14.8	28.3	51.2	68.6	80.7	87.3	88.5	84.3	74.7	59.7
DIC	19.6	37.3	67.1	89.5	104.5	112.1	112.2	104.9	90.1	67.9
TC	22.7	42.6	74.5	95.7	106.1	105.8	94.7	72.9	40.4	/
SDS	5.3	10.3	19.3	26.8	33.0	37.8	41.3	43.4	44.1	43.4
IL1	9.0	17.1	30.5	40.2	46.2	48.4	46.9	41.6	32.7	20.0
IL2	17.6	33.4	59.6	78.7	90.6	95.3	92.8	83.2	66.3	42.3
PLB	10.8	20.1	34.4	42.9	45.6	42.5	33.6	18.9	/	/

between the measured value and the predicted value of IA. It can be seen from Fig. 1 that the deviation degree between of the IA CRCs and measured CRCs has been changing in the whole concentration range, indicating that the joint action strength of mixtures has been changing. For example, SDS+DIC showed obvious synergistic effect in low concentration region ($\leq EC_{40}$), additive effect in medium concentration ranges (EC_{40} – EC_{60}) and antagonism in high concentration region. The Cd²⁺+DPH showed slight synergism in the low concentration region ($< EC_{20}$), additive effect in the medium and high concentration region ($> EC_{20}$). The changes of the interaction mode were reflected in 28 mixtures, such as Zn²⁺+CAP, Zn²⁺+SDBS, Cd²⁺+PLB, SDBS+DPH, DQ+IL1 etc. In order to obtain the joint action strength of binary mixtures in the whole concentration range, EC_{10} and EC_{20} were selected as representatives of low concentration range, EC_{50} of medium concentration range, and EC_{70} of high concentration range (Chen et al., 2019). Based on the prediction results of IA, the strength of joint actions at four representative concentrations was calculated by $rMDR_x$ model, as shown in Table S2. According to Table 2 and Table S2, The characteristic parameters of components in the three groups of Zn²⁺+TC, CAP+DPH and CAP+SDS are similar, and their joint action is additive. It is further verified that the substances with similar CRCs have additive effect (Wang et al., 2018). The DPH+SDS combination with similar characteristic parameters appears abnormal phenomenon. The low concentration of DPH+SDS is the additive effect, and the high concentration shows more than 50% synergistic effect. This is directly related to the white emulsion of the mixture in the medium and high concentration ranges in the experiment, which affects the experimental results. The 11 mixtures with a joint effect greater than 50% are: Zn²⁺+Cd²⁺, Zn²⁺+DQ, Zn²⁺+IL2, Cd²⁺+DQ, Cd²⁺+DIC, SDBS+DPH, SDBS+PLB, CAP+IL2, DIC+PLB, IL1+IL2 and IL1+PLB, and the $\Delta(k \cdot EC_{50})\%$ of mixtures are: 142.2%, 41.2%, 34.4%, 99.8%, 95.7%, 45.1%, 80.6%, 80.1%, 56.9%, 79.9%, and 51.5%.

3.5. The relationship between the joint action of binary mixtures and $\Delta(k \cdot EC_x)\%$

The relationship between the $\Delta(k \cdot EC_x)\%$ and the $rMDR_x$ of each mixture was fitted according to the method described in Section 2.6. The results show that the relationship of them can be well fitted by exponential function (Equ. 9). All the Adj.R² values were higher than 0.94. The Red.Chi-S values were lower than 100, except for 303 for the DQ+TC. The fitting equation is shown in Table S3, and the fitting curves are shown in Fig. 2 which includes Figs. 2.1–2.4.

Fig. 2 shows the relationship between $\Delta(k \cdot EC_x)\%$ and the $rMDR_x$ of binary mixtures from low concentration to high concentration. As $|\Delta(k \cdot EC_x)\%|$ increases, $|rMDR_x|$ also increases, and the function is identified as an increasing function; on the contrary, as $|\Delta(k \cdot EC_x)\%|$ increases, $|rMDR_x|$ decreases, and the function is identified as a decreasing function. To facilitate curve analysis, auxiliary dotted lines $rMDR_x = 0$ and $\Delta(k \cdot EC_x)\% = 0$ were drawn respectively. For example, the PLB+DPH: $rMDR_x$ varied from -40 – 0 , that is, the antagonistic strength varied from

0% to 40%. The exponential function is divided into two sections by $\Delta(k \cdot EC_x)\% = 0$. In the interval $[-100, 0]$, with the decrease of $|\Delta(k \cdot EC_x)\%|$, the antagonistic strength increased from 0% to 32%, which was a decreasing function. In the interval $[0, 80]$, with the increase of $|\Delta(k \cdot EC_x)\%|$ from 0% to 80%, the antagonistic strength increased from 32% to 46%, which was an increasing function.

There are 21 mixtures which CRCs trend changes ($\Delta(k \cdot EC_x)\% > 0$ and $\Delta(k \cdot EC_x)\% < 0$) in the whole concentration range. 12 of them change the mode of joint action (both antagonistic and synergistic effects existed) and were named a₁, as shown in Fig. 2.1. In a₁ type, all of them are non-monotonic functions, and the intersection of dotted line $rMDR_x = 0$ and $\Delta(k \cdot EC_x)\% = 0$ with exponential function does not coincide. But the mixture concentration corresponding to the intersection point of the dotted line $rMDR_x = 0$ and the exponential function is lower (10 groups are consistent with this situation). In other words, the change of the joint action mode of the mixture is much earlier than the change of shape of the component CRCs. An interesting phenomenon is found: whether the joint action is antagonistic or synergetic, the function is divided into three segments by two intersections of the dotted line $rMDR_x = 0$ or $\Delta(k \cdot EC_x)\% = 0$ with the exponential function dividing the function into three sections, from low concentration to high concentration – increasing function, decreasing function, increasing function respectively (except for IL2+DQ, the function value of high concentration region is unchanged). That is to say, with the increase of $|\Delta(k \cdot EC_x)\%|$, the strength of joint actions first increases, then decreases, and finally increases.

Fig. 2.2 shows the relationship between $\Delta(k \cdot EC_x)\%$ and the $rMDR_x$ of 9 mixtures named type a₂ (only antagonistic or synergistic action). In a₂ type, there are 2 groups of increasing functions and 3 groups of decreasing functions (all synergetic), and 4 groups of non-monotonic function. In 4 groups of non-monotonic functions, the dotted line $\Delta(k \cdot EC_x)\% = 0$ divides the exponential function into two segments. When the joint action was antagonistic, from low concentration to high concentration they are decreasing function and increasing function respectively. That is to say, with the increase of $|\Delta(k \cdot EC_x)\%|$, the strength of joint actions first decreases and then increases. While the joint action is synergetic, exactly the opposite, i.e. with the increase of $|\Delta(k \cdot EC_x)\%|$, the strength of joint action first increases and then decreases.

There are 45 mixtures which CRCs trend doesn't change ($\Delta(k \cdot EC_x)\% > 0$ or $\Delta(k \cdot EC_x)\% < 0$) in the whole concentration range. 19 of them change the mode of joint action and were named b₁, as shown in Fig. 2.3. In b₁ type, they are all non-monotonic functions, and the dotted line $rMDR_x = 0$ divides the exponential function into two sections. When $\Delta(k \cdot EC_x)\% > 0$, from low concentration to high concentration they are decreasing function and increasing function. That is to say, with the increase of $\Delta(k \cdot EC_x)\%$, the strength of joint action first decreases and then increases. When $\Delta(k \cdot EC_x)\% < 0$, the trend is exactly the opposite. That is to say, with the increase of $|\Delta(k \cdot EC_x)\%|$, the strength of joint action first increases and then decreases. This law has nothing to do with the joint action mode of the mixture.

The other 26 mixtures don't change the mode of joint action and

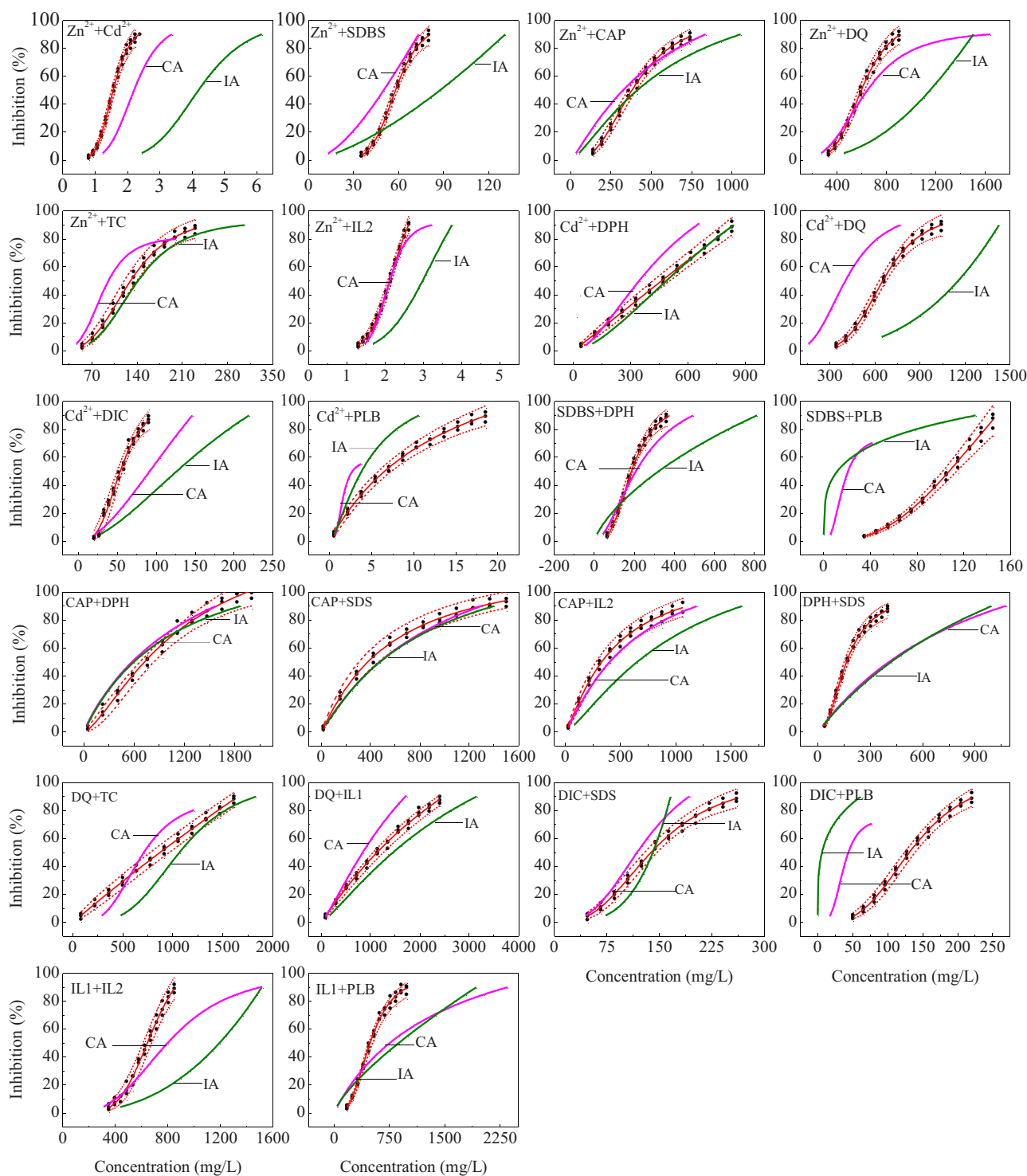


Fig. 1. Prediction of binary mixture joint action IA and CA models is mentioned in this paper. Exposure time: 15 min. Black dots (●): Observed data; red solid lines (—): Hill model fit, the dashed lines (---): 95% confidence intervals; red solid lines (—): CRC predicted by CA; the green solid lines (—): CRC predicted by IA. (For interpretation of the references to colour in this figure legend, the reader is referred to the web version of this article.)

were named b_2 , as shown in Fig. 2.4. In b_2 type, they are all monotone function. Among them, 14 groups show synergistic action (7 groups of increasing function and 7 groups of decreasing function) and 12 groups of antagonistic action (7 groups of increasing function and 5 groups of decreasing function). In this case, the probability of the mixtures producing antagonism or synergism is close, and the probability of the antagonism or synergism presenting an increasing function is close to that of a decreasing function.

$\Delta(k \cdot EC_x)\%$ can be directly obtained from the dose-response equation of the substances, and with a few toxicity test data of low, medium and high concentrations, the joint toxicity of binary mixtures in the whole concentration range can be predicted.

4. Conclusions

The single and binary acute toxicity of 12 kinds of environmental

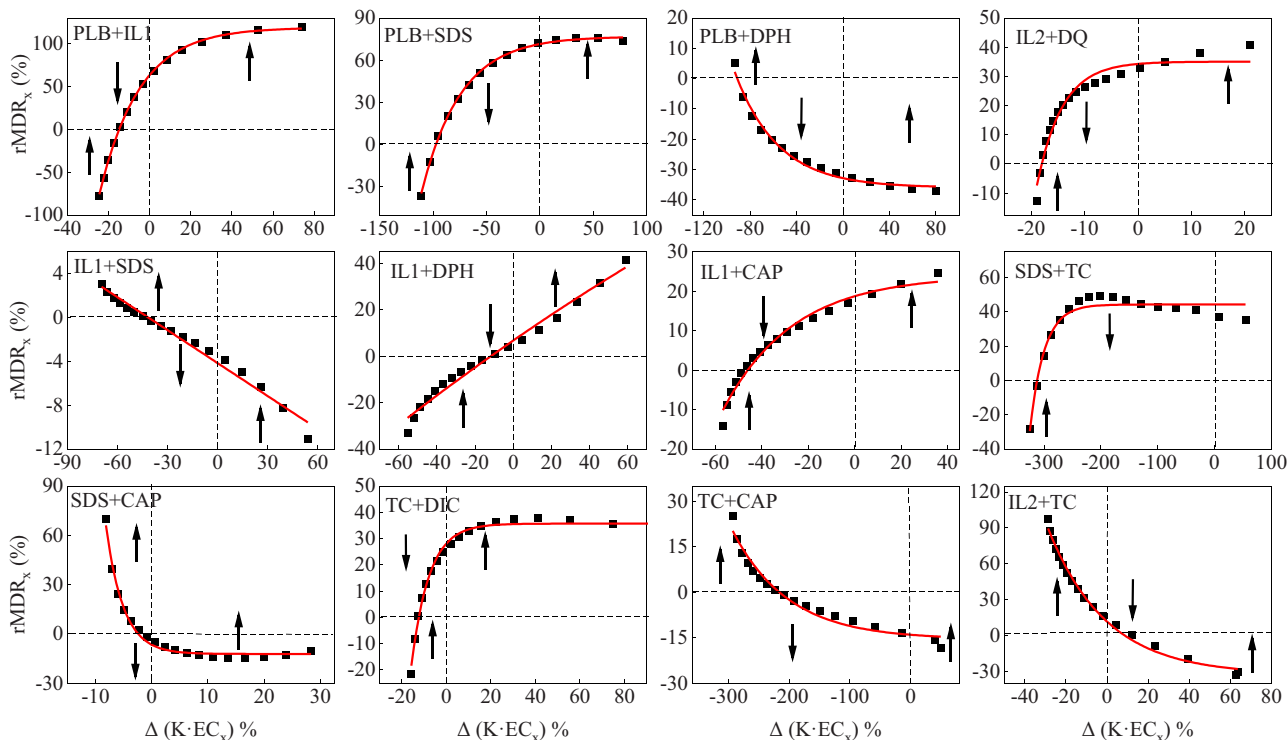


Fig. 2.1. The fitting curves of $\Delta(k \cdot EC_x)\%$ and $rMDR_x$ (a_1 type). The black dots (●): Experimental value; the red solid lines (—): Exponential model fit; increasing function, decreasing function. a_1 : $\Delta(k \cdot EC_x)\% > 0$ and $\Delta(k \cdot EC_x)\% < 0$, $rMDR_x > 0$ and $rMDR_x < 0$. (For interpretation of the references to colour in this figure legend, the reader is referred to the web version of this article.)

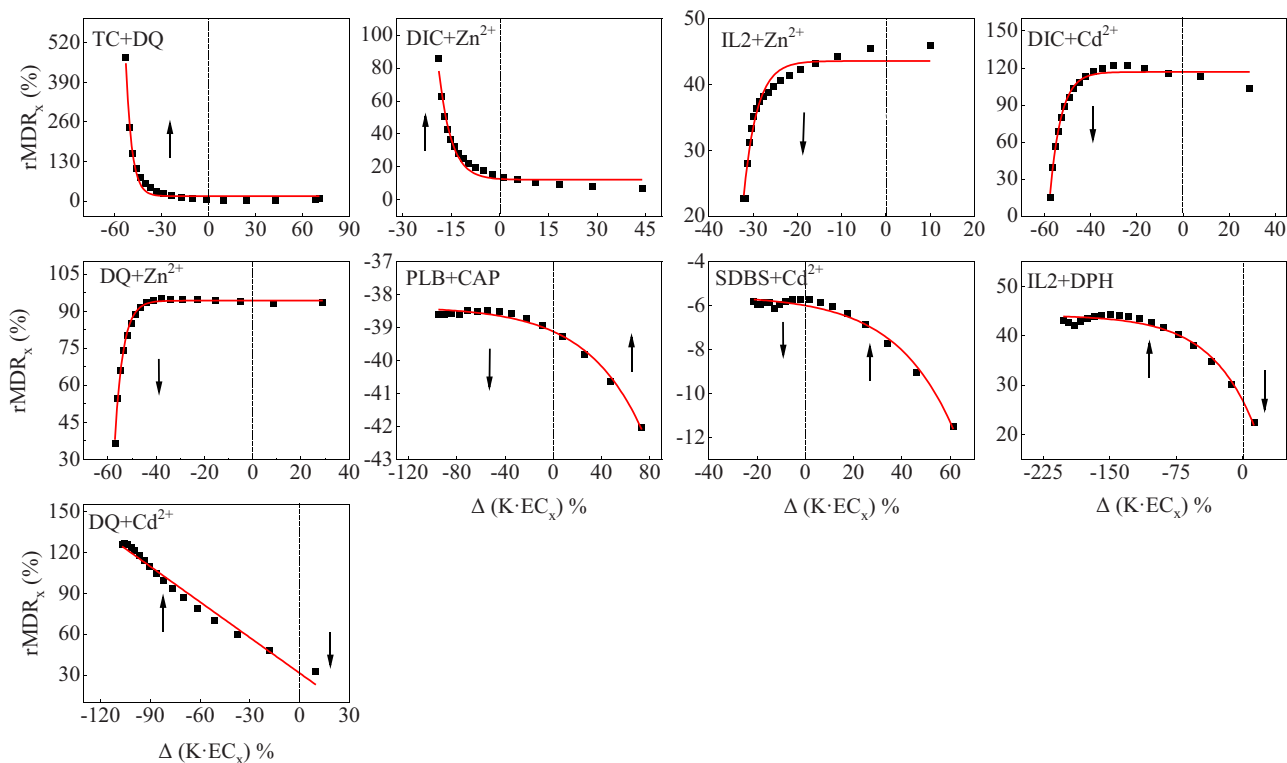


Fig. 2.2. The fitting curves of $\Delta(k \cdot EC_x)\%$ and $rMDR_x$ (a_2 type). The black dots (●): Experimental value; the red solid lines (—): Exponential model fit; increasing function, decreasing function. a_2 : $\Delta(k \cdot EC_x)\% > 0$ and $\Delta(k \cdot EC_x)\% < 0$, $rMDR_x > 0$ or $rMDR_x < 0$. (For interpretation of the references to colour in this figure legend, the reader is referred to the web version of this article.)

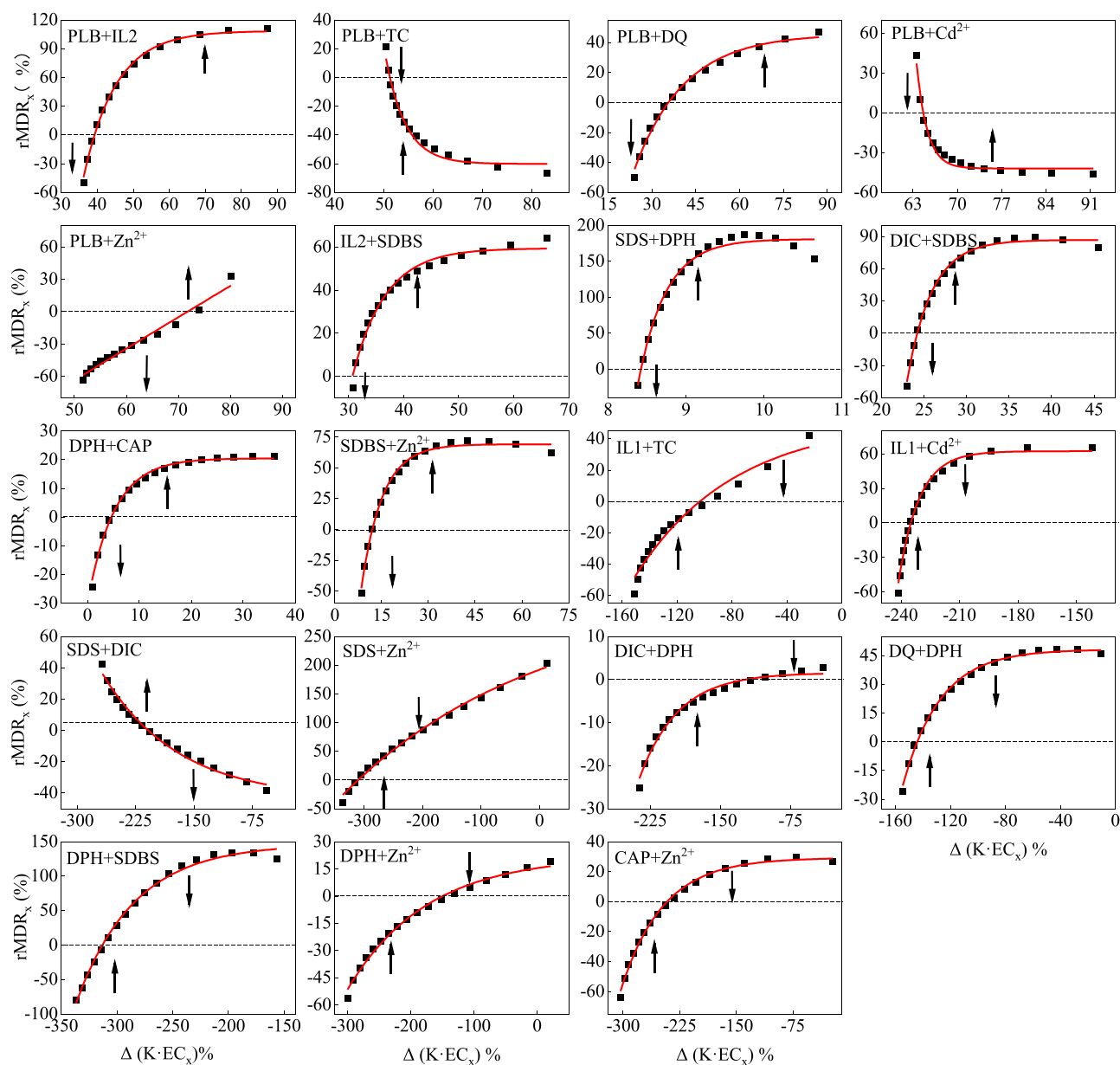


Fig. 2.3. The fitting curves of $\Delta(k \cdot EC_x)\%$ and $rMDR_x$ (b_1 type). The black dots (●): Experimental value; the red solid lines (—): Exponential model fit.: increasing function,.: decreasing function. b_1 : $\Delta(k \cdot EC_x)\% > 0$ or $\Delta(k \cdot EC_x)\% < 0$, $rMDR_x > 0$ and $rMDR_x < 0$. (For interpretation of the references to colour in this figure legend, the reader is referred to the web version of this article.)

pollutants from different sources to *Vibrio fischeri* was tested by micro-plate assay. The toxicity order of the twelve tested substances was $Zn^{2+} > IL2 > Cd^{2+} > PLB > SDBS > SDS > DIC > TC > DPH > CAP > IL1 > DQ$. The parameter n of the fitting equation varies from 3.12 to 6.50, which indicates that the CRCs shapes of the tested substance are quite different. The change order of characteristic parameter $k \cdot EC_x$ is basically the same as that of parameter n , and it can describe the shape of CRCs in the whole concentration range in detail.

The toxicity of 66 binary mixtures was analyzed by CA and IA models, 65% of the mixtures produced strong antagonism or synergism effects. According to the experimental results and the analysis of related literature, IA model is the best model to predict the joint action of binary mixtures among the two models. EC_{10} , EC_{20} , EC_{50} , EC_{70} were selected as representative concentrations, and IA model and modified $rMDR$ model were used to evaluate the strength of joint effect for binary mixtures. It is found that $Zn^{2+}+TC$, $CAP+DPH$, $CAP+SDS$ with similar $k \cdot EC_x$ all show additive effect. The $\Delta(k \cdot EC_x)\%$ of mixtures whose average joint action

strength is greater than 50% at four representative concentrations are greater than 34.4%. The difference of $k \cdot EC_x$ of each component in the mixture is the cause of joint action. The exponential function can well characterize the relationship between $\Delta(k \cdot EC_x)\%$ and $rMDR_x$.

By analyzing the fitting curve of $rMDR_x$ and $\Delta(k \cdot EC_x)\%$, it is found that: (1) For a_1 type binary mixtures, the change of joint action mode is earlier than the change of CRCs shape. With the increase of $|\Delta(k \cdot EC_x)\%|$, the strength of joint action first increases, then decreases and then increases, which is not related to the mode of joint action. (2) For a_2 type binary mixtures, when the fitting exponential functions are monotonic, the interaction is likely to be synergistic. When the fitting exponential functions are non-monotonic and the joint action is antagonistic, with the increase of $|\Delta(k \cdot EC_x)\%|$, the strength of joint action first decreases and then increases. When the joint action is synergetic, the trend is exactly the opposite. (3) For b_1 type binary mixtures, when $\Delta(k \cdot EC_x)\% > 0$, with the increase of $\Delta(k \cdot EC_x)\%$, the joint action strength first decreases and then increases. When $\Delta(k \cdot EC_x)\% < 0$, with the increase of

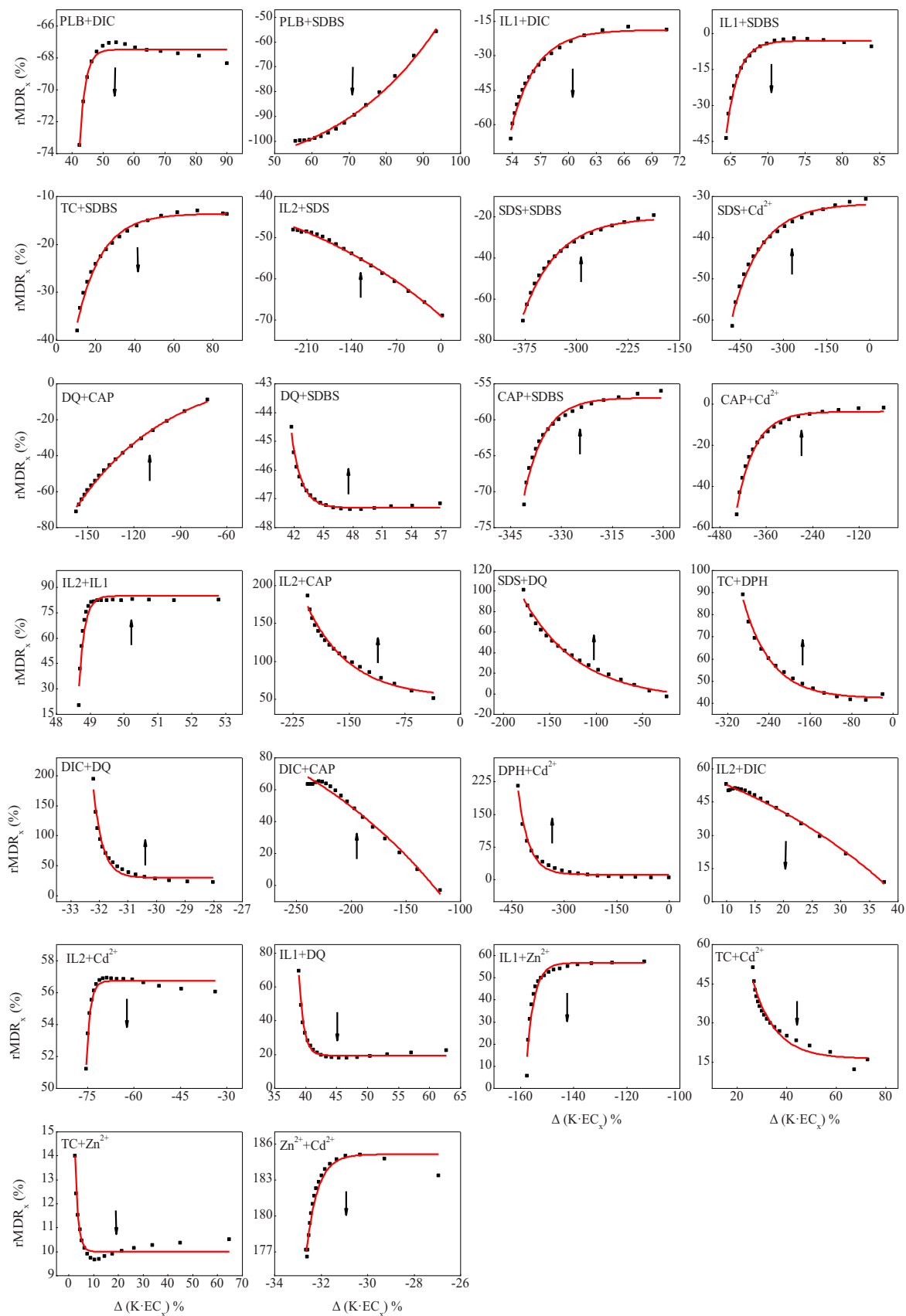


Fig. 2.4. The fitting curves of $\Delta(k \cdot EC_x)\%$ and $rMDR_x$ (b_2 type). The black dots (●): Experimental value; the red solid lines (—): Exponential model fit.: increasing function,.; decreasing function. b_2 : $\Delta(k \cdot EC_x)\% > 0$ or $\Delta(k \cdot EC_x)\% < 0$, $rMDR_x > 0$ or $rMDR_x < 0$. (For interpretation of the references to colour in this figure legend, the reader is referred to the web version of this article.)

$[\Delta(k \cdot EC_x)\%]$, the trend is exactly the opposite. This rule is applicable to both antagonistic and synergistic effects. (4) For b_2 type binary mixtures, the fitting exponential functions are all monotone functions and the probability of increasing and decreasing functions is similar, regardless of the mode of action.

This study reveals the relationship between the joint toxicity (mode and strength) of binary mixtures and the shape of CRCs of components, and obtains the variation rule of joint toxicity with parameter $\Delta(k \cdot EC_x)\%$. Following the rule, very important data can be obtained in the individual toxicity experiment, and the joint toxicity of binary mixture can be predicted to a certain extent. It provides theoretical support for the prediction of joint effects of mixtures from the view of geometry. The applicability of this rule in binary mixtures with different concentration ratios and multicomponent mixtures is also a topic for the future study.

CRedit authorship contribution statement

Wang Na: Conceptualization, Methodology, Validation, Investigation Writing - original draft, Writing - review & editing, Supervision, Resources, Funding acquisition. **Sun Ruru:** Data curation, Validation, Formal analysis, Investigation, Visualization. **Wang Xiaochang:** Writing - review & editing. **Ma Xiaoyan:** Project administration, Writing - review & editing. **Zhou Jinhong:** Investigation.

Declaration of Competing Interest

The authors declare that they have no known competing financial interests or personal relationships that could have appeared to influence the work reported in this paper.

Acknowledgments

The work is supported by the National Natural Science Foundation of China [grant No. 51708447]. Some of the toxicity tests were carried out in the Key Lab of Northwest Water Resource, Environment and Ecology, MOE, China.

Appendix A. Supporting information

Supplementary data associated with this article can be found in the online version at [doi:10.1016/j.ecoenv.2021.112155](https://doi.org/10.1016/j.ecoenv.2021.112155).

References

- Altenburger, R., Walter, H., Grote, M., 2004. What contributes to the combined effect of a complex mixture? *Environ. Sci. Technol.* 38, 6353–6362.
- Arrhenius, Å., Grönvall, F., Scholze, M., Backhaus, T., Blanck, H., 2004. Predictability of the mixture toxicity of 12 similarly acting congeneric inhibitors of photosystem II in marine periphyton and epipsammon communities. *Aquat. Toxicol.* 68, 351–367.
- Belden, J.B., Gilliom, R.J., Lydy, M.J., 2007. How well can we predict the toxicity of pesticide mixtures to aquatic life? *Integr. Environ. Assess.* 3, 364–372.
- Bellas, J., 2008. Prediction and assessment of mixture toxicity of compounds in antifouling paints using the sea-urchin embryo-larval bioassay. *Aquat. Toxicol.* 88, 308–315.
- Bliss, C.I., 1939. The toxicity of poisons applied jointly. *Ann. Appl. Biol.* 26, 585–615.
- Brezovšek, P., Eleršek, T., Filipič, M., 2014. Toxicities of four anti-neoplastic drugs and their binary mixtures tested on the green alga *Pseudokirchneriella subcapitata* and the cyanobacterium *Synechococcus leopoliensis*. *Water Res.* 52, 168–177.
- Cedergreen, N., Christensen, A.M., Kamper, A., Kudsk, P., Mathiassen, S.K., Streibig, J.C., Sørensen, H., 2008. A review of independent action compared to concentration addition as reference models for mixtures of compounds with different molecular target sites. *Environ. Toxicol. Chem.* 27, 1621–1632.
- Chen, Y.H., Qin, L.T., Mo, L.Y., Zhao, D.N., Zeng, H. Hu, Liang, Y.P., 2019. Synergetic effects of novel aromatic brominated and chlorinated disinfection byproducts on *Vibrio qinghaiensis* sp.-Q67. *Environ. Pollut.* 250, 375–385.
- Cui, D., Mebel, A.M., Arroyo-Mora, L.E., Zhao, C., De Caprio, A., O'Shea, K., 2018. Fundamental study of the ultrasonic induced degradation of the popular antihistamine, diphenhydramine (DPH). *Water Res.* 144, 265–273.
- Diaz, E., Monsalvo, V.M., Lopez, J., Mena, I.F., Palomar, J., Rodriguez, J.J., 2018. Assessment of the ecotoxicity and inhibition of imidazolium ionic liquids by respiration inhibition assays. *Ecotoxicol. Environ. Saf.* 162, 29–34.
- Dou, R.N., Liu, S.S., Liu, H.L., Wang, L.J., Qin, L.T., 2010. Toxicities of binary mixtures including at least one component with J-shaped dose-response curve. *Asian J. Ecotoxicol.* 5, 498–504 (in Chinese).
- Ge, H.L., Liu, S.S., Su, B.X., Qin, L.T., 2014. Predicting synergistic toxicity of heavy metals and ionic liquids on photobacterium Q67. *J. Hazard. Mater.* 268, 77–83.
- Hass, U., Scholze, M., Christiansen, S., Dalgaard, M., Vinggaard, A.M., Axelstad, M., Metzendorf, S.B., Kortenkamp, A., 2007. Combined exposure to anti-androgens exacerbates disruption of sexual differentiation in the rat. *Environ. Health Perspect.* 115, 122–128.
- Kar, S., Leszczynski, J., 2019. Exploration of computational approaches to predict the toxicity of chemical mixtures. *Toxics* 7, 15.
- Kortenkamp, A., Backhaus, T., Faust, M., 2009. State of the Art Report on Mixture Toxicity. Report for Directorate General for the Environment of the European Commission.
- Liu, S.S., Song, X.Q., Liu, Hai, L., Zhang, Y.H., Zhang, J., 2009. Combined photobacterium toxicity of herbicide mixtures containing one insecticide. *Chemosphere* 75, 381–388.
- Liu, S.S., Liu, L., Chen, F., 2013. Application of the concentration addition model in the assessment of chemical mixture toxicity. *Acta Chim. Sin.* 71, 1335–1340 (in Chinese).
- Liu, T., Zhu, L.S., Wang, J.H., Wang, J., Xie, H., 2015. The genotoxic and cytotoxic effects of 1-butyl-3-methylimidazolium chloride in soil on *Vicia faba* seedlings. *J. Hazard. Mater.* 285, 27–36.
- Loewe, S., 1926. Effect of combinations: mathematical basis of problem. *Arch. Exp. Pathol. Pharmacol.* 114, 313–326.
- Ma, X.Y., Wang, Y.K., Dong, K., Wang, X.C., Zheng, K., Hao, L.W., Ngo, H.H., 2019. The treatability of trace organic pollutants in WWTP effluent and associated biotoxicity reduction by advanced treatment processes for effluent quality improvement. *Water Res.* 159, 423–433.
- Mo, L.Y., Qin, R.Q., Qin, L.T., Zeng, H.H., Liang, Y.P., 2015. Study on the quantitative relationship between the structure and toxicity of organophosphorus pesticide. *Chin. J. Struct. Chem.* 34, 1473–1478 (in Chinese).
- Mwene, M., Wang, X.Z., Buontempo, F.V., Horan, N., Young, A., Osborn, D., 2004. Prediction of noninteractive mixture toxicity of organic compounds based on a fuzzy set method. *J. Chem. Inf. Comput. Sci.* 44, 1763–1773.
- Olmstead, A.W., LeBlanc, G.A., 2005. Toxicity assessment of environmentally relevant pollutant mixtures using a heuristic model. *Integr. Environ. Assess.* 1, 114–122.
- Qin, L.T., Liu, S.S., Zhang, J., Xiao, Q.F., 2011. A novel model integrated concentration addition with independent action for the prediction of toxicity of multi-component mixture. *Toxicology* 280, 164–172.
- Qin, L.T., Wu, J., Mo, L.Y., Zeng, H.H., Liang, Y.P., 2015. Linear regression model for predicting interactive mixture toxicity of pesticide and ionic liquid. *Environ. Sci. Pollut. Res.* 22, 12759–12768.
- Qin, L.T., Zhang, X., Mo, L.Y., Liang, Y.P., Zeng, H.H., 2017. Further exploring linear concentration addition and independent action for predicting non-interactive mixture toxicity. *Chin. J. Struct. Chem.* 36 (6), 886–896 (in Chinese).
- Qin, L.T., Chen, Y.H., Zhang, X., Mo, L.Y., Zeng, H.H., Liang, Y.P., 2018. QSAR prediction of additive and non-additive mixture toxicities of antibiotics and pesticide. *Chemosphere* 198, 122–129.
- Rial, D., Vázquez, J.A., Mendiña, A., García, A.M., González, M.P., Mirón, J., Murado, M.A., 2013. Toxicity of binary mixtures of oil fractions to sea urchin embryos. *J. Hazard. Mater.* 263, 431–440.
- Tan, Y.M., Clewell, H., Campbell, Jerry, Andersen, M., 2011. Evaluating pharmacokinetic and pharmacodynamic interactions with computational models in supporting cumulative risk assessment. *Int. J. Environ. Res. Public Health* 8, 1613–1630.
- Wang, N., Wang, X.C., Ma, X.Y., 2015. Characteristics of concentration-inhibition curves of individual chemicals and applicability of the concentration addition model for mixture toxicity prediction. *Ecotoxicol. Environ. Saf.* 113, 176–182.
- Wang, N., Ma, X.Y., Wang, X.C., Zhang, X.Y., 2018. Preliminary study on the joint action based on the chemical dose-response curve shape. *J. Saf. Environ.* 18, 386–390 (in Chinese).
- Wang, X.D., Meng, X.Q., Ma, Y.B., Pu, X., Zhong, X., 2018. The prediction of combined toxicity of Cu-Ni for barley using an extended concentration addition model. *Environ. Pollut.* 242, 136–142.
- Wang, Z., Chen, J.W., Huang, L.P., Wang, Y., Cai, X.Y., Qiao, X.L., Dong, Y.Y., 2009. Integrated fuzzy concentration addition-independent action (IFCA-IA) model outperforms two-stage prediction (TSP) for predicting mixture toxicity. *Chemosphere* 74, 735–740.
- Wu, Q., Jin, Y., Zheng, H.X., Liu, X.T., 2010. The research progress of chloramphenicol and tetracycline inhibit bacterial protein secretion. *China Biotechnol.* 30, 97–100 (in Chinese).
- Yao, Z.F., Lin, Z.F., Wang, T., Tian, D.Y., Zou, X.M., Gao, Y., Yin, D.Q., 2013. Using molecular docking-based binding energy to predict toxicity of binary mixture with different binding sites. *Chemosphere* 92, 1169–1176.
- Yu, J., Cui, Y.Y., Zhang, H., Liu, Y., Oinuma, G., Yamauchi, T., Mu, Z., Yang, M., 2019. Degradation of SDBS in water solutions using plasma in gas-liquid interface discharge: performance, byproduct formation and toxicity evaluation. *Chemosphere* 234, 471–477.
- Zhan, Y.Z., Ma, N., Liu, R., Wang, N., Zhang, T., He, L.C., 2019. Polymyxin B and polymyxin E induce anaphylactoid response through mediation of Mas-related G protein-coupled receptor X2. *Chem-Biol. Interact.* 308, 304–311.
- Zhang, Q., Cheng, J.P., Xin, Q., 2015. Effects of tetracycline on developmental toxicity and molecular responses in zebrafish (*Danio rerio*) embryos. *Ecotoxicology* 24, 707–719.